

**Scaling behavior of $(N_{\text{ch}})^{-1}dN_{\text{ch}}/d\eta$ at $\sqrt{s_{\text{NN}}} = 130$ GeV by PHOBOS
Collaboration and its implication
— A possible explanation by the Ornstein-Uhlenbeck process —**

M. Biyajima¹, M. Ide¹, T. Mizoguchi² and N. Suzuki³

¹*Department of Physics, Faculty of Science, Shinshu University, Matsumoto
390-8621, Japan*

²*Toba National College of Maritime Technology, Toba 517-8501, Japan*

³*Matsusho Gakuen Junior College, Matsumoto 390-1295, Japan*

(Received February 12, 2019)

Recently interesting data on $dN_{\text{ch}}/d\eta$ in Au-Au collisions ($\eta = -\ln \tan(\theta/2)$) with the centrality cuts have been reported by PHOBOS Collaboration. Their data are usually divided by the number of participants (nucleons) in collisions. Instead of this way, using the total multiplicity $N_{\text{ch}} = \int (dN_{\text{ch}}/d\eta)d\eta$, we find that there is scaling phenomenon among $(N_{\text{ch}})^{-1}dN_{\text{ch}}/d\eta = dn/d\eta$ with different centrality cuts at $\sqrt{s_{\text{NN}}} = 130$ GeV. To explain this scaling behavior of $dn/d\eta$, we consider the stochastic approach named the Ornstein-Uhlenbeck process with two sources. The Langevin equation is adopted for the explanation. Moreover, comparisons of $dn/d\eta$ at $\sqrt{s_{\text{NN}}} = 130$ GeV with that at $\sqrt{s_{\text{NN}}} = 200$ GeV have been made. No significant difference has been found. Possible detection method of the quark-gluon plasma (QGP) through $dN_{\text{ch}}/d\eta$ is presented.

§1. Introduction

Recently PHOBOS Collaboration has published interesting data on $dN_{\text{ch}}/d\eta$ ($\eta = -\ln \tan(\theta/2)$)* in Au-Au collisions at $\sqrt{s_{\text{NN}}} = 130$ GeV¹. The authors of Ref. 1) have calculated the following quantity,

$$\frac{1}{\langle N_{\text{part}} \rangle / 2} \frac{dN_{\text{ch}}}{d\eta} = f(\langle N_{\text{part}} \rangle, N_{\text{coll}}, \eta), \quad (1.1)$$

where N_{part} and N_{coll} mean the number of participants (nucleons) and number of collision particles in Au-Au collisions. It depends on the centrality cuts. The function $f(N_{\text{part}}, N_{\text{coll}}, \eta = 0)$ is an increasing function of $\langle N_{\text{part}} \rangle$, as $\langle N_{\text{part}} \rangle$ increases.

In this paper, instead of Eq. (1.1), we consider the following physical quantity,

$$\frac{1}{N_{\text{ch}}} \frac{dN_{\text{ch}}}{d\eta} = \frac{dn}{d\eta}, \quad (1.2)$$

*)

$$y = \frac{1}{2} \ln \frac{E + p_z}{E - p_z} = \frac{1}{2} \ln \left[\frac{\sqrt{1 + m^2/p_t^2 + \sinh^2 \eta} + \sinh \eta}{\sqrt{1 + m^2/p_t^2 + \sinh^2 \eta} - \sinh \eta} \right] = \tanh^{-1} \left(\frac{p_z}{E} \right) \approx -\ln \tan(\theta/2) \equiv \eta.$$

$$\eta = \frac{1}{2} \ln \frac{p + p_z}{p - p_z}, \text{ and } \frac{dn}{d\eta} = \frac{p}{E} \frac{dn}{dy}, \text{ where } \frac{p}{E} = \frac{\cosh \eta}{\sqrt{1 + m^2/p_t^2 + \sinh^2 \eta}}.$$

where $N_{\text{ch}} = \int (dN_{\text{ch}}/d\eta)d\eta$, and $\int (dn/d\eta)d\eta = 1$. In Fig. 1, three sets of $dn/d\eta$'s are shown. They suggest that there is the scaling behavior among $dn/d\eta$'s with different centrality cuts. Thus $dn/d\eta$ is named a kind of the probability density, because the variable η is the continuous variable. This fact probably implies that the stochastic approach is available in analyses of $dn/d\eta$ **)

Contents of the present paper are as follows. In the second section, we examine the $dn/d\eta$ scaling. In §3, the stochastic approach is considered, as one of possible explanations for the $dn/d\eta$ scaling. In §4, concrete analyses by the Gaussian distributions obtained from the Ornstein-Uhlenbeck(O-U) process are presented. In the final section, concluding remarks are given.

§2. Confirmation of $dn/d\eta$ scaling

It is worth while to confirm whether $dn/d\eta$ scaling holds. Using the intercepts of $dn/d\eta$ at $\eta = 0$ in Fig. 1,

$$\left. \frac{dn}{d\eta} \right|_{\eta=0} = c \approx 0.129 \pm 0.005 \quad (2.1)$$

we can obtain a relation between N_{ch} and $\langle N_{\text{part}} \rangle$ as follows: The PHOBOS Collaboration has reported the following behaviors at $\eta = 0$,

$$\frac{1}{0.5\langle N_{\text{part}} \rangle} \left. \frac{dN_{\text{ch}}}{d\eta} \right|_{\eta=0} = A\langle N_{\text{part}} \rangle^\alpha \quad (2.2)$$

where $A = 2.16$, and $\alpha = 0.064$. Thus we obtain the following relation,

$$c = \frac{0.5\langle N_{\text{part}} \rangle}{N_{\text{ch}}} \frac{1}{0.5\langle N_{\text{part}} \rangle} \left. \frac{dN_{\text{ch}}}{d\eta} \right|_{\eta=0} = \frac{0.5\langle N_{\text{part}} \rangle}{N_{\text{ch}}} A\langle N_{\text{part}} \rangle^\alpha. \quad (2.3)$$

Equation (2.3) is examined in Table I and Fig. 2. That Eq. (2.3) holds approximately among 6 centrality cuts is reflecting the $dn/d\eta$ scaling, in particular, in the central region.

*) Multiplicity distributions in high energy collisions, i.e., $P(n, \langle n \rangle)$'s are the probability distributions, which are function of n and $\langle n \rangle$. It is known that the KNO scaling functions,

$$\lim_{n, \langle n \rangle \rightarrow \infty} \langle n \rangle P(n) = \psi(z = n/\langle n \rangle)$$

are described by solutions of various Fokker-Planck equations²⁾⁻⁴⁾.

**) Dokshitzer has calculated the generalized gamma distribution in QCD⁵⁾

$$P(z = n/\langle n \rangle) \approx \frac{2\mu^2}{z} \frac{(Dz)^{3\mu/2}}{\sqrt{2\mu\gamma}} \exp[-(Dz)^\mu],$$

where z , μ , D , γ are KNO scaling variable, $1 - \gamma = 1/\mu$, a parameter, the anomalous dimension in QCD, respectively. This is a steady solution of the following Fokker-Planck Equation

$$\frac{\partial P}{\partial t} = -\frac{\partial}{\partial z} \left[\left(d + \frac{1}{2}Q \right) z + bz^{1+\gamma} \right] P + \frac{1}{2}Q \frac{\partial^2}{\partial z^2} [z^2 P].$$

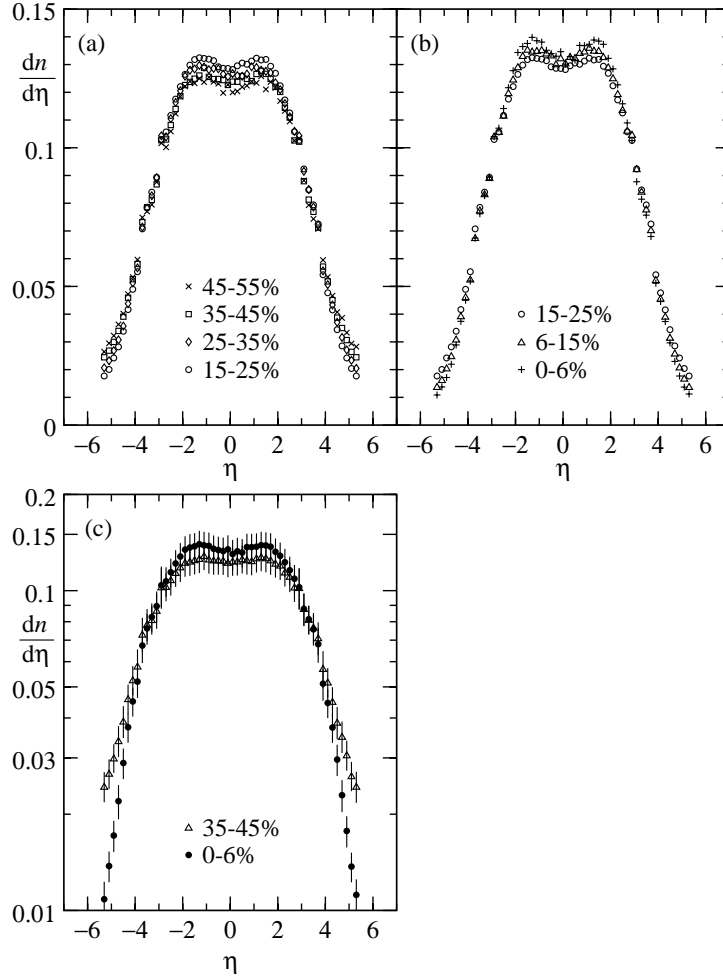


Fig. 1. (a) and (b) Two sets of $dn/d\eta$ with different centrality cuts¹⁾. Data with 15-25% are used in both Figures, for the sake of comparisons. (c) To examine $dn/d\eta$ in the fragmentation region the logarithmic axis is used.

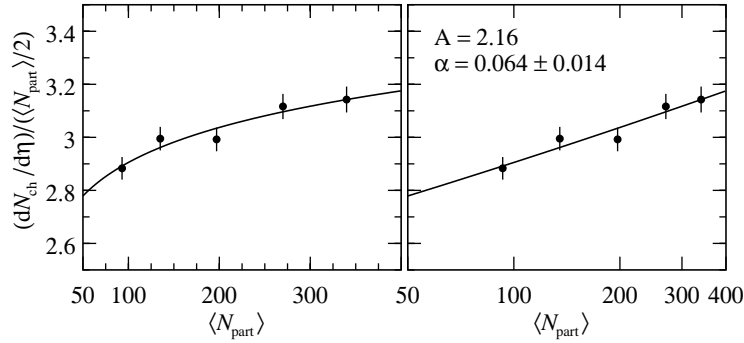
§3. A possible explanation of $dn/d\eta$ by stochastic approach

It is well known that the rapidity ($y \approx \eta$) is a kind of the velocity. Moreover, there are leading particles in the beam and target nuclei in collisions; nucleons in gold at RHIC experiments, collide each other, lose their energies and emit various particles. Since we have to treat large number of particles, $1k \sim 10k$, the stochastic approach seems to be one of useful tools.

To describe the $dn/d\eta$ scaling with the leading particle effect and the fluctuation in the rapidity space, we assume the following Langevin equation⁶⁾⁻⁸⁾ for the rapidity

Table I. Empirical examination of Eq. (2·3).

centrality (%)	$2c \times N_{ch}$	$A \times \langle N_{part} \rangle^{1+\alpha}$
35-45	$2 \times 0.129 \times 1056$ 272.6 ± 14.6	$2.16 \times 93^{1+0.064}$ 268.5 ± 17.7
25-35	$2 \times 0.129 \times 1582$ 408.1 ± 21.9	$2.16 \times 135^{1+0.064}$ 399.1 ± 28.4
15-25	$2 \times 0.129 \times 2270$ 585.7 ± 31.4	$2.16 \times 197^{1+0.064}$ 596.7 ± 45.8
6-15	$2 \times 0.129 \times 3199$ 825.2 ± 44.6	$2.16 \times 270^{1+0.064}$ 834.5 ± 67.9
0-6	$2 \times 0.129 \times 4070$ 1050 ± 57	$2.16 \times 340^{1+0.064}$ 1066 ± 90

Fig. 2. Estimation of parameters A and α .

variable*)

$$\frac{dy}{dt} = -\gamma y + f_w(t), \quad (3\cdot1)$$

where γ and $f_w(t)$ are the frictional coefficient and the white noise, respectively. In our treatment, that N_{ch} particles have been produced at $\pm y_{max}$ at $t = 0$ is assumed, moreover. This picture is corresponding to the leading particle effects. Using this assumption $y(0) = \pm y_{max}$, we obtain the following solution

$$y(t) = \pm y_{max} e^{-\gamma t} + e^{-\gamma t} \int_0^t e^{\gamma s} f_w(s) ds. \quad (3\cdot2)$$

The average quantity and the variance are calculated as

$$E[y(t)] = \pm y_{max} e^{-\gamma t}, \quad (3\cdot3)$$

$$E[(E[y(t)] - y)^2] = \frac{\sigma^2}{2\gamma} (1 - e^{-2\gamma t}), \quad (3\cdot4)$$

*) In classical mechanics, Eq. (3·1) corresponds to the following equation,

$$m \frac{dv}{dt} = -m\gamma v + m f_w(t),$$

where v is the velocity.

where we use the expression for the white noise,

$$\langle f_w(t)f_w(s) \rangle = \sigma^2\delta(t-s), \quad (3-5)$$

where σ^2 is the variance. It is known that the distribution function is described by the Gaussian distribution with the average quantity and the variance: The probability density with $V^2(t) = (\sigma^2/2\gamma)(1 - e^{-2\gamma t})$ is expressed as

$$P(y, y_{\text{max}}, t) = \frac{1}{\sqrt{8\pi V^2(t)}} \left\{ \exp \left[-\frac{(y + y_{\text{max}}e^{-\gamma t})^2}{2V^2(t)} \right] + \exp \left[-\frac{(y - y_{\text{max}}e^{-\gamma t})^2}{2V^2(t)} \right] \right\}. \quad (3-6)$$

The connection between Eq. (3-1) and the Fokker-Planck equation for the O-U process is given in Appendix.

In Fig. 3(a), we depict a simplified picture of heavy-ion collision. Our assumptions for the leading particle effect is equivalent to the assumption $0.5 \times \delta(y - y_{\text{max}})$ and $0.5 \times \delta(y + y_{\text{max}})$ at $t = 0$. In other words, as this model with two sources is very simple, $0.5 \times N_{\text{ch}}$ particles at y_{max} and the same $0.5 \times N_{\text{ch}}$ particles at $-y_{\text{max}}$ have produced at $t = 0$. The evolution of Eq. (3-6) is shown in Fig. 3(b).

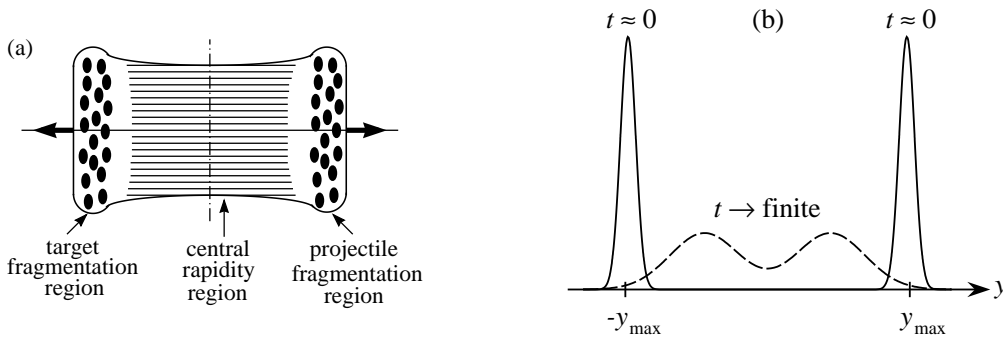


Fig. 3. (a) Simplified picture for A-A collisions. Thin line denotes partons. The black circles mean nucleons. (b) Evolution of Eq. (3-6) with two sources at y_{max} and $-y_{\text{max}}$.

§4. Analyses of $dn/d\eta$ by means of Eq. (3-6)

By making use of Eq. (3-6), we can analyse $dn/d\eta$ shown in Fig. 1. In our calculation, as most of produced particles are not specified, we assume that $y \approx \eta$ in Eq. (3-6). Our results are shown in Fig. 4 and Table II. In Fig. 5, we examine whether or not the variance $V^2(t)$ and $p = 1 - e^{-2\gamma t}$ depend on the centrality cuts. As is seen in Figs. 3 and 4, the scaling behavior among $dn/d\eta$'s at $\sqrt{s_{\text{NN}}} = 130$ GeV is explained by Eq. (3-6) with small changes in the variance $V^2(t)$. The values of the variance $V^2(t)$ depend on the distribution in the fragmentation region $[-\eta_{\text{max}} < \eta < -4$ and $4 < \eta < \eta_{\text{max}}]$. It can be said that the scaling behavior is explained fairly well by the O-U process with two sources at the beam (y_B or y_{max})

and target (y_T or $-y_{\max}$) rapidities. Of course, we have examined that the single source cannot explain it*).

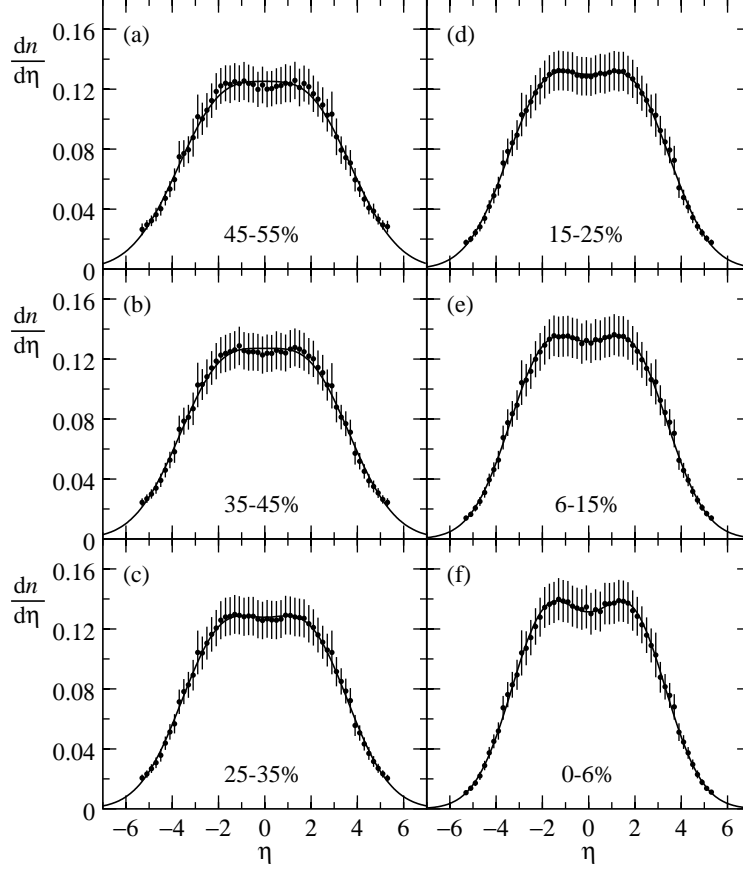


Fig. 4. Analyses of $dn/d\eta$ by Eq. (3-6). See Table II.

Table II. Estimated parameters in our analyses by Eq. (3-6) with two sources. Evolution of Eq.

(3-6) is stopped at minimum χ^2 's. $\delta p = 0.006 \sim 0.004$. $c = \frac{1}{\sqrt{2\pi V^2(t)}} \exp\left[-\frac{(y_{\max} e^{-\gamma t})^2}{2V^2(t)}\right]$

Fig. 4	(a)	(b)	(c)	(d)	(e)	(f)
centrality (%)	45-55	35-45	25-35	15-25	6-15	0-6
p	$0.872 \pm \delta p$	$0.875 \pm \delta p$	$0.878 \pm \delta p$	$0.882 \pm \delta p$	$0.886 \pm \delta p$	$0.888 \pm \delta p$
$V^2(t)$	3.83 ± 0.27	3.61 ± 0.21	3.23 ± 0.16	3.00 ± 0.13	2.72 ± 0.10	2.47 ± 0.08
$\langle N_{\text{part}} \rangle$	—	93	135	197	270	340
N_{ch}	662 ± 10	1056 ± 16	1582 ± 23	2270 ± 34	3199 ± 49	4070 ± 63
c	0.125	0.127	0.128	0.130	0.132	0.131
$\chi^2/n.d.f.$	8.61/51	7.63/51	5.88/51	5.35/51	3.57/51	3.82/51

*) For an explanation with the single source at $y_0 \approx 0$, we can use Eq. (A-2) in Appendix. Our result for the centrality cut 0-6 %, we obtain $\chi^2 = 25.76$ with $m/p_t = 1.3 \pm 0.1$, which is necessary for the single source model. If m/p_t is neglected, we obtain worse χ^2 . Thus we disregard this model.

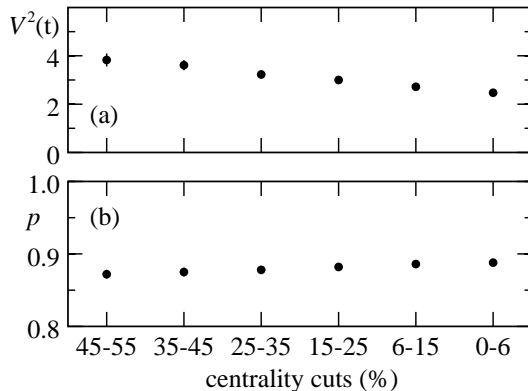


Fig. 5. Variance $V^2(t)$ and p of Fig. 4 and Table II.

The intercepts of $dn/d\eta$'s are calculated by the following expression,

$$c = \frac{1}{\sqrt{2\pi V^2(t)}} \exp \left[-\frac{(y_{\text{max}} e^{-\gamma t})^2}{2V^2(t)} \right] \quad (4.1)$$

The results are shown in Table II. They are almost the same as values in Fig. 1.

Here we should carefully examine $V(t)$ in Table II. The slight change is reflecting the discrepancies in the fragmentation region. As is seen in Fig. 1(c), there are small differences in $dn/d\eta$'s over the range $|\eta| \gtrsim 4$ between centrality cut 0-6% and others. To explore the differences more carefully, we need $dn/d\eta$ with smaller centrality cuts, 0-3% \sim 0-5%^{*)**}.

§5. Concluding remarks

First of all, it can be said that there is the scaling among $dn/d\eta$'s with various centrality cuts at $\sqrt{s_{\text{NN}}} = 130$ GeV, because of constant c 's values and behaviour of Fig. 1(a)~(c).

Second the scaling behavior of $dn/d\eta$ is described by the solution of the Langevin equation with two sources, i.e., Eq. (3.6)^{***}. See Fig. 4 and c 's values in Table II.

^{*)} The calculation based on QCD has been done in Ref. 9) as

$$\frac{2}{\langle N_{\text{part}} \rangle} \frac{dN_{\text{ch}}}{d\eta} \Big|_{\eta=0} = a \left(\frac{s}{s_0} \right)^{\lambda/2} \left[\log \left(\frac{Q_{0\text{S}}^2}{\Lambda_{\text{QCD}}^2} \right) + \frac{\lambda}{2} \log \left(\frac{s}{s_0} \right) \right]$$

where $a \approx 0.82$, $\Lambda_{\text{QCD}} = 0.2$ GeV, $\lambda = 0.25$ and the centrality dependence of the saturation scale $Q_{0\text{S}}^2$. In the fragmentation region this expression needs the cutoff factors.

^{**) Very recently the BRAHMS COllaboration^{10), 11)} has reported the $dn/d\eta$ at $\sqrt{s_{\text{NN}}} = 130$ GeV, and 200 GeV with centrality cuts 0-5% and others. We have analysed them by Eq. (3.6) and obtained almost the constant $V^2(t)$'s, because the data in the fragmentation region are lacking at $|\eta| \gtrsim 4.5$.}

^{***)} To estimate the ‘‘thermalization time’’ of the QGP, Hwa has considered the Fokker-Planck equation for the motion of the quarks and gluons in nuclei¹²⁾. See also Ref. 13) in which the Wiener process is considered for the problem on the thermalization of the quarks and gluons.

Moreover, we can add the following fact. Very recently, PHOBOS Collaboration has reported the data on $dN_{\text{ch}}/d\eta$ with centrality cut 0-6% at $\sqrt{s_{\text{NN}}} = 200$ GeV¹⁴⁾. They are compared with $dn/d\eta$ at $\sqrt{s_{\text{NN}}} = 130$ GeV in Fig. 6. It is obvious that the scaling on $dn/d\eta$ holds between $\sqrt{s_{\text{NN}}} = 130$ GeV and 200 GeV*).

This suggests that $dn/d\eta$ with the centrality cut 0-6% do not show singular /or particular phenomenon relating to signatures of the Quark-Gluon Plasma (QGP). Of course, we should pay our attention that we are handling the averaged quantity in statistics. At present, however, it is difficult to conclude that the QGP is created, and the signatures from the QGP are washed out by the strong interactions between hadrons, if the QGP is created.

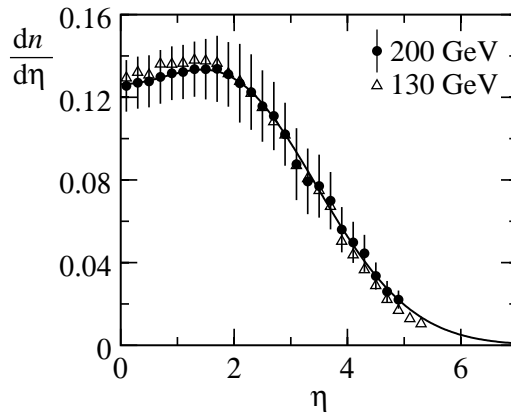


Fig. 6. Comparisons of $dn/d\eta$ with the centrality cut 0-6% at $\sqrt{s_{\text{NN}}} = 130$ GeV and 200 GeV. Solid line is obtained for latter energy: $p = 0.879 \pm 0.007$, $V^2(t) = 2.67 \pm 0.24$, $\chi^2/n.d.f = 0.63/22$, $c = 0.126$.

To investigate the particular phenomena like the turbulence and/or deflagration in $dN_{\text{ch}}/d\eta$, we need to analyse the single event with smaller centrality cut than 0-6%.

Moreover, analyses of event-by-event by means of the intermittency¹⁶⁾⁻²¹⁾ and the wavelet²²⁾ is necessary to investigate the detections of the QGP and the Disoriented Chiral Condensate(DCC). For the latter case, the ratio of neutral pion ($\langle\pi^0\rangle$) to the charged pions ($\langle\pi^{\text{ch}}\rangle$), $\langle\pi^0\rangle/\langle\pi^{\text{ch}}\rangle$ should be measured. These methods should be applied to $dN_{\text{ch}}/d\eta$ with smaller centrality cuts and larger particles. They seem to be available to draw useful information on the QGP and DCC from the analyses of single events.

*) Using the Bjorken's picture¹⁵⁾ for the calculation of energy density near $|\Delta\eta| \leq 0.5$ with the geometrical picture of the gold ($R_\tau \approx 6-7$ fm, $c\tau_0 \approx 1-2$ fm, $V \approx \pi R_\tau^2(c\tau_0) \approx 300$ fm³), we obtain the following values

$$\begin{aligned} \varepsilon &\sim \frac{3}{2} \frac{1}{V} \frac{dN_{\text{ch}}}{d\eta} E_T \Big|_{|\Delta\eta| \leq 0.5} \sim 1 \text{ GeV/fm}^3 \quad (130 \text{ GeV}), \\ \varepsilon &\sim 1.2 \text{ GeV/fm}^3 \quad (200 \text{ GeV}). \end{aligned}$$

Acknowledgements

One of authors (M. B.) is partially indebted to the Japanese Grant-in-aid for Education, Science, Sports and Culture (No. 09440103). Conversation with S. Raha is greatly acknowledged.

Appendix

The Fokker-Planck equation for the Ornstein-Uhlenbeck process connected with Eq. (3.1) is given as

$$\frac{\partial P(y, t)}{\partial t} = \gamma \left[\frac{\partial}{\partial y} y + \frac{1}{2} \frac{\sigma^2}{\gamma} \frac{\partial^2}{\partial y^2} \right] P(y, t). \quad (\text{A}\cdot 1)$$

The solution of Eq. (A.1) with $\delta(y - y_0)$ at $t = 0$ is obtained as

$$P(y, t) = \frac{1}{\sqrt{2\pi V^2(t)}} \exp \left[-\frac{(y - y_0 e^{-\gamma t})^2}{2V^2(t)} \right], \quad (\text{A}\cdot 2)$$

where we use a resolution method for partial differential equation²³⁾. The solution of Eq. (A.1) with $\delta(y \pm y_{\text{max}})$ at $t = 0$ is obtained as

$$P(y, y_{\text{max}}, t) = \frac{1}{\sqrt{8\pi V^2(t)}} \left\{ \exp \left[-\frac{(y + y_{\text{max}} e^{-\gamma t})^2}{2V^2(t)} \right] + \exp \left[-\frac{(y - y_{\text{max}} e^{-\gamma t})^2}{2V^2(t)} \right] \right\}. \quad (\text{A}\cdot 3)$$

References

- 1) B. B. Back *et al.* [PHOBOS Collaboration], Phys. Rev. Lett. **87** (2001) 102303.
- 2) Z. Koba, H. B. Nielsen and P. Olesen, Nucl. Phys. B **40** (1972) 317.
- 3) M. Biyajima, Phys. Lett. **137B** (1984) 225 [**140B** (1984) 435].
- 4) M. Biyajima, Phys. Lett. B **139** (1984) 93; See Also, P. Carruthers and C. C. Shih, Int. J. Mod. Phys. A **2** (1987) 1447.
- 5) Y. L. Dokshitzer, Phys. Lett. B **305** (1993) 295.
- 6) N. G. van Kampen, "Stochastic Processes in Physics and Chemistry", (North-Holland Publ., Amsterdam, 1981).
- 7) K. Saitou, "Probability and Stochastic Process for Engineers" (in Japanese), (Saiensu-Sya, Tokyo, 1980).
- 8) J. Hori, "Langevin Equation" (in Japanese), (Iwanami-Shoten, Tokyo, 1982).
- 9) D. Kharzeev and E. Levin, Phys. Lett. B **523**, 79 (2001).
- 10) I. G. Bearden *et al.* [BRAHMS Collaborations], Phys. Lett. B **523**, 227 (2001)
- 11) I. G. Bearden *et al.* [BRAHMS Collaboration], arXiv:nucl-ex/0112001.
- 12) R. C. Hwa, Phys. Rev. D **32** (1985) 637.
- 13) S. Chakraborty and D. Syam, Lett. Nuovo Cim. **41** (1984) 381.
- 14) B. B. Back *et al.* [PHOBOS Collaboration], arXiv:nucl-ex/0108009.
- 15) J. D. Bjorken, Phys. Rev. D **27** (1983) 140.
- 16) T. H. Burnett *et al.*, Phys. Rev. Lett. **50** (1983) 2062.
- 17) F. Takagi, Phys. Rev. Lett. **53** (1984) 427.
- 18) A. Bialas and R. Peschanski, Nucl. Phys. B **273** (1986) 703.

- 19) M. Biyajima, A. Bartl, T. Mizoguchi and N. Suzuki, Phys. Lett. B **237** (1990) 563 [Addendum-ibid. B **247** (1990) 629].
- 20) I. V. Andreev, M. Biyajima, I. M. Dremin and N. Suzuki, Int. J. Mod. Phys. A **10** (1995) 3951.
- 21) R. C. Hwa, "Quark - Gluon Plasma," (World Scientific, Singapore, 1990), 665.
- 22) N. Suzuki, M. Biyajima and A. Ohsawa, Prog. Theor. Phys. **94** (1995) 91; See also, N. Suzuki, M. Biyajima and A. Ohsawa, Nucl. Phys. Proc. Suppl. **52B** (1997) 246.
- 23) N. S. Goel and N. Richter-Dyn, "Stochastic Models in Biology", (Academic Press, New York, 1974).